IMPLEMENTATION AND VERIFICATION OF NUMERICAL MODEL FOR GAS BUBBLE DYNAMICS IN ELECTROCONDUCTIVE FLUID

A. Tucs[(1)], S. Spitans[(1,2)], A. Jakovics[(1)], E. Baake[(2)], B. Nacke[(2)]

[(1)] Laboratory for Mathematical Modeling of Environmental and Technological Processes, University of Latvia, Zellu Str. 8, LV-1002 Riga, Latvia
[(2)] Institute of Electrotechnology, Leibniz University of Hannover, Wilhelm-Busch Str. 4, 30167 Hannover, Germany

ABSTRACT. Apart from common steam reforming process the thermal decomposition of methane is regarded as an alternate route to producing hydrogen and elemental carbon with out of CO_2 emissions. Chemical reaction of decarburation can be ensured by means of methane bubbly flow through a molten metal bath and additionally controlled by external electromagnetic field.

The aim of this research is to develop and verify the numerical model for the gas bubble dynamics in molten metal bath and, using the developed approach, to tailor external AC/DC EM field in order to meet the maximal efficiency of reactor.

This is the initial stage of research and preliminary calculation results for the single bubble rise dynamics in 2D axisymmetric consideration at different flow conditions and 2D planar consideration in the presence of external DC EM field are obtained and compared to experimental and simulation data from literature.

INTRODUCTION

Hydrogen production without carbon dioxide formation appears to be highly attractive not only in terms of refraining and reducing of CO_2 emissions that cause greenhouse effects, but also for substituting non-renewable fossil fuels in the variety of combustion applications they are serving nowadays.

One of the possibilities to produce H_2 without forming CO_2 is to carry decomposition of CH_4 to solid carbon and H_2 [1]:

$$CH_4 \rightarrow C + 2H_2, (\Delta H = 74.85 \text{ kJ/mol}).$$

Because reaction of decarburation is endothermic the temperature must be above 600 °C for reaction to proceed at a reasonable rate. For example, such conditions for chemical reaction can be achieved by ensuring a methane bubbly flow through a molten metal bath.

Meanwhile, optimal parameters for methane bubble size, velocity and residence time in the bath can be additionally adjusted by the AC/DC electromagnetic (EM) field combination.

The main objective of this long-term research is by means of existing Eulerian-Eulerian [2] and Eulerian-Lagrangian [3] techniques to develop and verify the numerical model for the gas bubble dynamics in EM induced flow of molten metal and, using the developed approach, to tailor external EM field in order to meet conditions for the maximal efficiency of reactor.

FORMER RESEARCH

Apart from the bubble cloud behavior, rather complex is even a single bubble rise dynamics. Hence basic principles of particular bubble emersion must be understood in order to develop an accurate numerical model for simulation of the whole methane thermal cracking reactor (Figure 1). In general case, system that consists of liquid phase and gas inclusions can be completely described with four non-dimensional parameters:

$$Ar = \left(\rho_l \cdot g^{0.5} \cdot D^{1.5}\right) / \mu_l \,, \tag{1}$$

$$Bo = Eo = \left(\rho_l \cdot g \cdot D^2\right) / \sigma \,, \tag{2}$$

$$\rho_l / \rho_b \,, \tag{3}$$

$$\mu_l / \mu_b \,, \tag{4}$$

where ρ_l and ρ_b is density of liquid and gas, g - gravitational acceleration, D - diameter of the bubble, μ_l and μ_b - viscosity of liquid and gas, σ - surface tension. Archimedes number (Ar) characterizes buoyancy and viscous force ratio, while Bond (Bo) or Eotvos (Eo) number describes the ratio between the buoyancy and the surface tension force. Using Archimedes number there can also be defined Reynolds number Re:

$$Re = Fr \cdot Ar \,. \tag{5}$$

Fr stands for the Froude number and is defined as

$$Fr = U_\infty / \left(g \cdot D\right)^{0.5} \,, \tag{6}$$

where U_∞ is terminal velocity of the rising bubble. Frequently in experimental investigations there is also used the Morton number M:

$$M = \left(g \cdot \mu_l^4\right) / \left(\rho_l \cdot \sigma^3\right) . \tag{7}$$

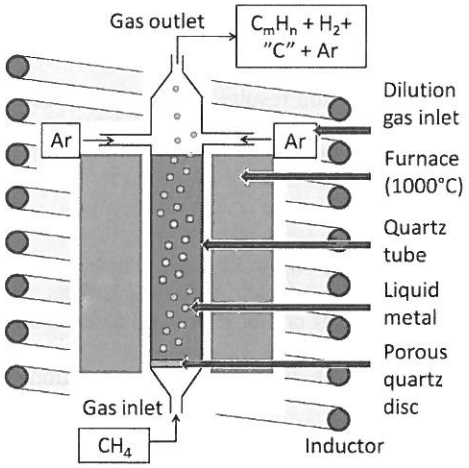

Figure 1. Liquid metal bubbly column for H_2 production without CO_2 emission.

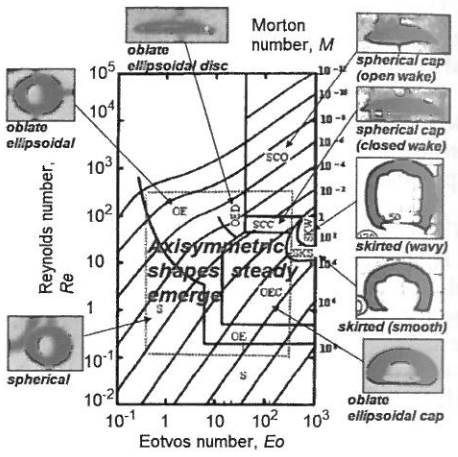

Figure 2. Classification of experimentally observed steady rising bubble shapes [4].

The terminal shapes of single rising bubble in a water column at a range of Ar and Bo numbers were observed and reported in the work [4] as shown in Figure 2. Generally, small bubbles that have low Re or Bo numbers ($Re < 1$ or $Bo < 1$) rise in a steady fashion and maintain the spherical shape. The shape of larger bubbles at intermediate Re and Bo numbers ($1 < Re < 100$ and $1 < Bo < 100$) are significantly affected by the flow conditions. Various bubble shapes (oblate ellipsoid, disk-like, oblate ellipsoidal cap, skirt and spherical-cap) have been found in various flow regimes by the experimental investigations. In spite of the difference in shapes the bubbles emerge steadily along a straight path. With the further increase of Re number ($100 < Re < 500$) regime, the bubble shape may become torroidal at the great Bo number values ($100 < Bo < 500$); spherical-cap in intermediate Bond number regime ($30 < Bo < 100$) and oblate ellipsoid in the low Bond number regime ($1 < Bo < 30$). As the bubble size increases further, turbulent wake develops behind the bubble that leads to

unsteady bubble motion. The bubble may rise in a wobbly manner, oscillate about the mean shape and even break up and coalesce. In general, the rising bubbles have axisymmetric shapes when the non-dimensional numbers are not higher ($Re < 200$, $Bo < 200$) within the range indicated by the dot in Figure 2.

Bubble rise dynamics can be considered in 2D system like Hele-Shaw cell and it is found that the path of a circular air bubble rising in a viscous fluid change to a zig-zag path when the *Re* number of bubble exceeds a threshold [5]. At greater *Bo* numbers this process is accompanied also with shape oscillations. With increase of *Ar* number the coupling between wake dynamics, bubble path and shape oscillations evolves and succession of contrasted oscillation regimes is observed [6].

There also can be considered a bubble rise in liquid metal in the presence of external EM field. In this case because the bubble is electrically non-conductive the magnetic field should affect the bubble motion indirectly through the changes in the liquid flow structure. In the work [7] argon bubble rise in GaInSn eutectic under the influence of a DC longitudinal magnetic field (parallel to the main direction of bubble motion) was experimentally investigated and suppression of liquid velocity oscillations in the bubble wake was observed (the same effect is observed in case of conductive liquid flow around an insulating cylinder with external magnetic field parallel to the flow direction [8]). It was also found that the field influence on bubble movement is strongly depended on the bubble size: for small bubbles ($D < 4.6$ mm) an increase of the drag coefficient with increasing magnetic interaction parameter was observed, whereas for larger bubbles ($D > 5.4$ mm) the application of the magnetic field reduced the drag coefficient. In general, due to the lack of suitable experimental capabilities to determine the bubble shape, so far there exists only a numerical model prediction: bubble will elongate in the direction of the field [9].

RISING BUBBLE MODEL

Governing equations

Bubble rise dynamics in electrically conductive liquid in external DC EM field can be characterized by the following set of equations:

$$\nabla^2 \vec{B} / (\mu_0 \sigma_l) + (\vec{B} \cdot \nabla)\vec{U} - (\vec{U} \cdot \nabla)\vec{B} = 0, \tag{8}$$

$$\vec{j} = \sigma_l \left(-\nabla\varphi + \left[\vec{U} \times \vec{B}\right]\right), \tag{9}$$

$$\nabla \cdot \vec{U} = 0, \tag{10}$$

$$\frac{\partial \vec{U}}{\partial t} + (\vec{U} \cdot \nabla)\vec{U} = -\frac{1}{\rho_l}\nabla p + \nu_l \nabla^2 \vec{U} + \vec{f}, \tag{11}$$

where $\vec{B}$ is magnetic field induction, μ_0 - magnetic constant, σ_l - electrical conductivity of liquid, $\vec{U}$ - velocity, p - pressure, ν_l - kinematic viscosity, $\vec{f}$ - sum of volume forces, e. g. gravitational $\vec{f}_g = \vec{g}$ and Lorentz force $\vec{f}_{Lor} = (\vec{j} \times \vec{B}) / \rho_l$ ($\vec{j}$ - current density). First pair of equations describes EM nature of the process: Amperes circuital law (8), where displacement currents are neglected, and Ohm's law (9).

The second pair of equations denotes on hydrodynamic processes of conductive viscous liquid that is considered as incompressible (10). Momentum balance is achieved on account of equation (11).

Because the system contains two phases a dynamics of their boundary should also be described. This can be done by means of Volume of Fluid (VOF) technique implemented in *ANSYS Fluent* or Level-Set (L-S) method in *Comsol Multiphysics*.

Volume of Fluid technique

Phase distribution can be characterized by a phase field function $VF(r_i, t)$ (i^{th} mesh element is given a scalar value *VF*). If mesh element does not contain melt then $VF = 0$, otherwise -

VF = 1 and mesh element is completely filled with melt. And when the phase interface crosses mesh element - 0 < VF < 1. In general, interface dynamics is characterized by the following transport equation:

$$\frac{\partial VF}{\partial t} + \vec{U} \cdot \nabla (VF) = 0 . \qquad (12)$$

Level-Set method

The Level-Set interface finds the fluid interface by tracking the isolines of the level set function ϕ. Isocontour ϕ = 0.5 determines the position of the interface. The equation governing the evolution of ϕ is

$$\frac{\partial \phi}{\partial t} + \vec{U} \cdot \nabla (\phi) = \gamma \nabla \cdot \left(\varepsilon \nabla \phi - \phi(1-\phi) \frac{\nabla \phi}{|\nabla \phi|} \right), \qquad (13)$$

where γ (m/s) and ε (m) are reinitialization parameters. The parameter ε determines the thickness of the layer around the interface where ϕ goes from zero to one ($\varepsilon = h_c/2$, where h_c is the characteristic mesh size in the region passed by interface). The γ parameter determines the amount of reinitialization (a suitable value for γ is the maximum velocity magnitude occurring in the model).

Numerical simulation of single bubble rise in a viscous liquid in general is a great challenge because of variety of factors that should be taken into account to obtain physically correct results: numerical smearing of the interface between phases; discontinuity of physical properties across liquid interface that may lead to numerical instability; handling the geometry of deformable interface; complex physics on the interface, e.g. effects of surfactants. All these facts are dependent on the mesh quality and in majority of cases also significantly increase calculation time.

BUBBLE FREE EMERSION

On the basis of VOF numerical technique 2D axisymmetric model verification was performed. A bubble rise dynamics in axisymmetric domain ($R = 4 \cdot D_{bubble}$, $H = 12 \cdot D_{bubble}$) at different Archimedes and Bond number values was considered. Obtained terminal bubble shapes show good agreement with experiments [4] and results of existing numerical models [10] (Figure 3).

In numerical simulations and also in experiments, the visual observations of a bubble bottom indicate on a rounded lower edge for lower Ar numbers and sharper edge with the increase of Ar number.

Bubble shapes calculated by numerical models are in good agreement with experimental results. However, for the case of Bo = 116 and Ar = 206.3 the axisymmetric models predict torroidal bubble shape [10]. The authors show that it is caused by bubble initialization with unrealistic spherical shape in the beginning of the simulation.

Due to our interest in bubble dynamics in liquid metal a verification of model at $Bo \approx Bo_{GaInSn}$ = 1.87 and maximally allowed for axisymmetry assumption Ar = 200 was performed. In this case also a qualitative agreement between obtained bubble terminal shapes and existing numerical predictions [10] (Figure 4) was obtained.

Investigation of bubble rise dynamics using 2D model showed bubble path instability (Figure 5). For t < 0.0833s bubble path trajectory appears to be a straight line, but for t > 0.0833 s bubble motion becomes zig-zag type and it is accompanied by vortex shedding. Consideration of a "reverse" problem - the liquid flows around a rigid cylinder - a Karman vortex street is observed. Comparison between obtained results and experimental observations [5,6] proves a good qualitative agreement (Figure 6,7(a)). From bubble rise regime diagram (Figure 7, b) it can be concluded that in appropriate Archimedes number range the numerical simulation predicts instability that it is also observed in experiment.

Experiments		Simulations		
Test conditions	Observed bubble steady shapes [4]	Literature [10]	Axisymmetric model	Modeling conditions
$Eo = 8.67$ $M = 711$ $Re = 0.078$	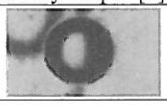			$Bo = 8.67$ $Ar = 0.98$
$Eo = 17.7$ $M = 711$ $Re = 0.232$	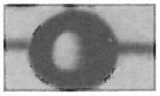			$Bo = 17.7$ $Ar = 1.67$
$Eo = 32.2$ $M = 0.00082$ $Re = 55.3$	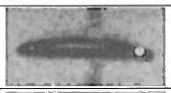			$Bo = 32.2$ $Ar = 79.88$
$Eo = 243$ $M = 266$ $Re = 7.77$	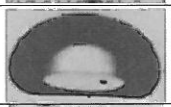	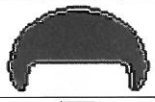	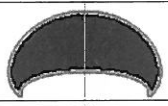	$Bo = 243$ $Ar = 15.24$
$Eo = 116$ $M = 848$ $Re = 2.47$			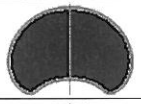	$Bo = 116$ $Ar = 6.55$
$Eo = 116$ $M = 266$ $Re = 3.57$			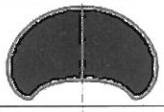	$Bo = 116$ $Ar = 8.75$
$Eo = 116$ $M = 41.1$ $Re = 7.16$	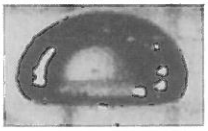		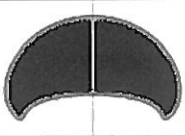	$Bo = 116$ $Ar = 13.95$
$Eo = 116$ $M = 5.51$ $Re = 13.3$	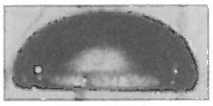		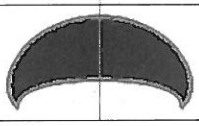	$Bo = 116$ $Ar = 23.6$
$Eo = 116$ $M = 0.0046$ $Re = 94.0$	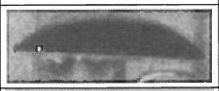			$Bo = 116$ $Ar = 135.4$
$Eo = 116$ $M = 0.00086$ $Re = 151$	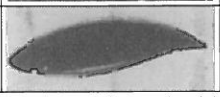			$Bo = 116$ $Ar = 206.3$

Figure 3. Comparison of terminal bubble shapes observed in experiments [4] and predicted in simulations ([10]/present model) for different Archimedes and Bond numbers.

Bo	Simulations ($Ar = 200$)	
	Literature [10]	Axisymmetric model
1	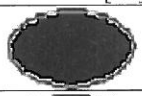	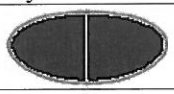
5		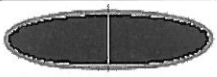

Figure 4. Comparison of terminal bubble shapes observed in simulations ([10]/present model) at $Bo \approx Bo_{GaInSn} = 1.87$.

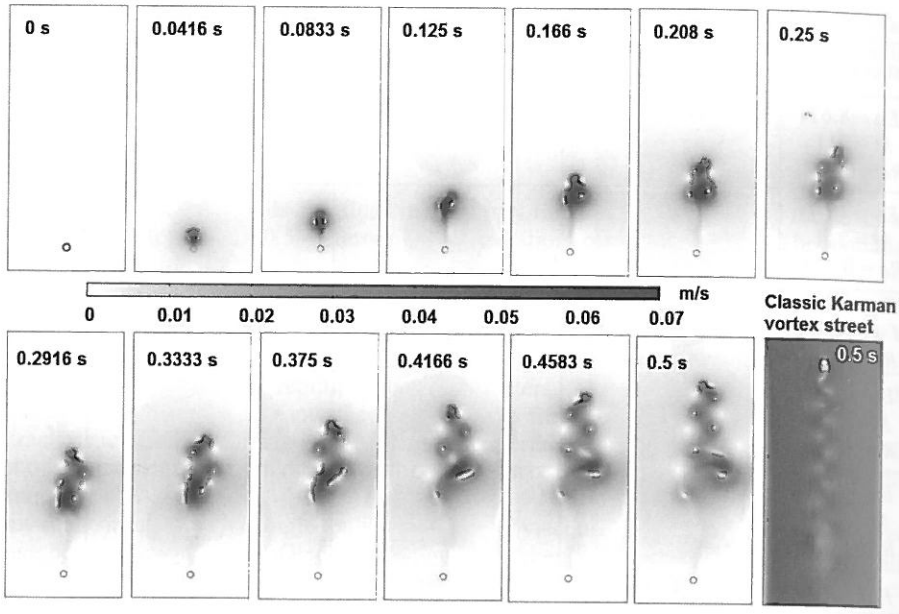

Figure 5. Rising bubble path instability evolution in Hele-Shaw cell (Bo = 8.67, Ar = 177.1, D_{bubble} = 0.8 mm, Domain = 16·50 mm^2) and qualitative comparison with Karman vortex street (v_{inlet} = 0.07 m/s, $D_{cylinder}$ = 0.8 mm).

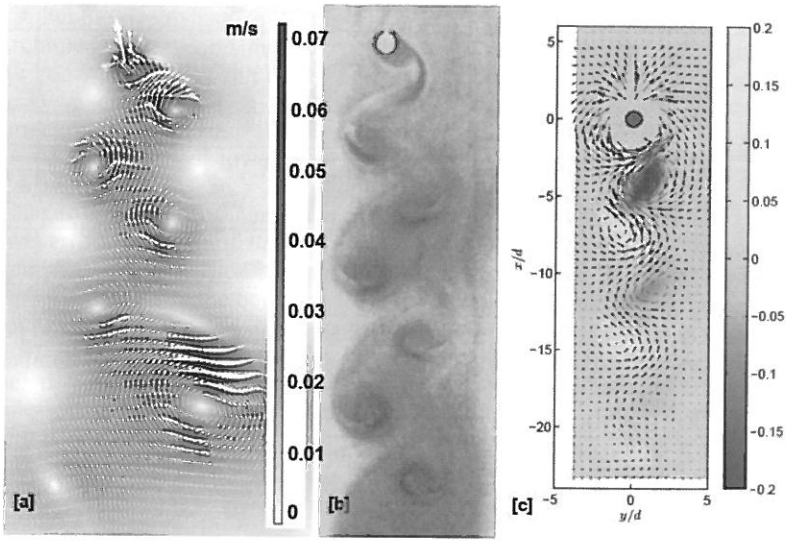

Figure 6. Path instability qualitative comparison. (a) Numerical observation (velocity field, Bo = 8.67, Ar = 177.1); (b) Experimental observation [5] (Bo ~ 1.8, Ar ~ 686); (c) Experimental observation [6] (velocity/vorticity field, Bo = 0.3, Ar = 200).

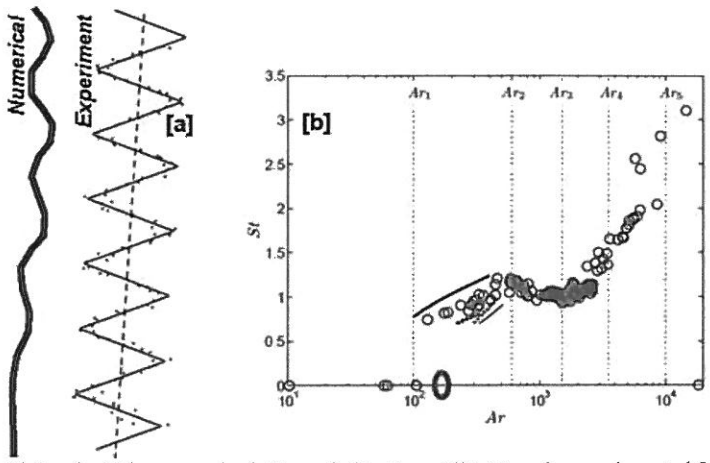

Figure 7. (a) Rising bubble numerical (Bo = 8.67, Re = 177.1) and experimental [5] (Bo ~ 1.8, Ar ~ 686) trajectory qualitative comparison. (b) Strouhal/Archimedes number diagram (experiment [6]), circle correspond numerical observation.

BUBBLE EMERSION IN A DC MAGNETIC FIELD

By means of coupling between magnetohydrodynamic module and VOF technique in *ANSYS Fluent* the developed numerical model was further verified for the case of 2D planar air (ρ_{air} = 1.2 kg/m^3, η_{air} = 18 μPa·s) bubble emersion in InGaSn eutectic (ρ_{InGaSn} = 6350 kg/m^3, σ_{InGaSn} = 3 MS/m, η_{InGaSn} = 1.9 mPa·s) in the presence of external DC magnetic field B_y oriented in the y direction of bubble rise.

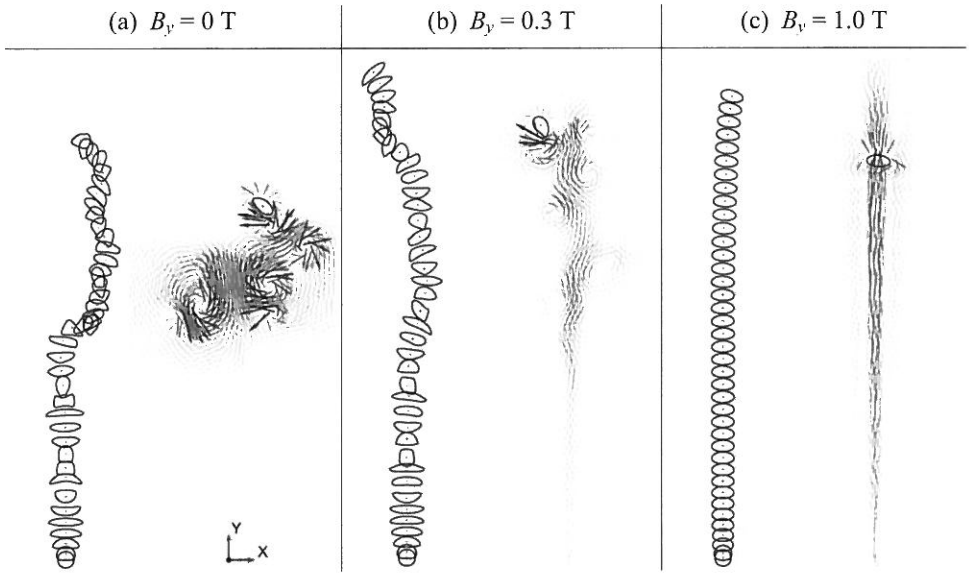

Figure 8. 2D planar simulation results for air bubble emersion (a) - with out of external axial DC magnetic field B_y = 0 T and in the presence of (b) - B_y = 0.3 T and (c) - B_y = 1.0 T. Bubble shapes are traced every 20 ms (on the left) and instantaneous flow pattern (0 - 27 cm/s) is given for the time moment t = 660 ms (on the right).

The spherical bubble with D_{bubble} = 4 mm diameter was initialized at the bottom of rectangular fluid domain ($x = 15 \cdot D_{bubble}$ and $y = 33 \cdot D_{bubble}$) in the beginning of calculation. Three cases were considered: bubble rise with out of EM field (Figure 8, a) and bubble emersion in weaker B_y = 0.3 T (Figure 8, b) and stronger B_y = 1.0 T (Figure 8, c) fields.

The obtained preliminary results (Figure 8) clearly show that with the increase of B_y the zig-zag trajectory in the purely hydrodynamic case becomes more rectilinear and vortical structures in the bubble wake, as well as intense bubble shape oscillations, are considerably damped and appear to be in good qualitative agreement with the previous experimental studies [7,8].

CONCLUSIONS

Verification of developed axisymmetric model for rising bubble description at appropriate flow conditions has proved good agreement with experimental [4] and existing numerical [10] results. Observed bubble path instability in Hele-Shaw system in characteristic parameter range qualitatively describes experimental results [5,6]. Applied longitudinal DC EM field suppresses path instability and vortex structures and appears to be in good qualitative agreement with experimental observations [7,8]. The model will be developed further and used for future studies of bubble ansamble dynamics in electrically conductive liquids in external AC/DC EM field combinations.

ACKNOWLEDGEMENTS

Current research was performed with financial support of the LIMTECH project and the European Social Fund within the project Nr. 2011/0002/2DP/2.1.1.1.0/10/APIA/VIAA/085 at the University of Latvia.

REFERENCES

[1] Abanades, A. (2011). Experimental analysis of direct thermal methane cracking. *Int. Journal of Hydrogen Energy*, 36, 12877-12886.

[2] Miao, X., Lucas, D., Ren, Z., Eckert, S., Gerbeth, G. (2013). Numerical modeling of bubble-driven liquid metal flows with external static magnetic field. *J. Comput. Phys.*, 48, 32-45.

[3] Ščepanskis, M., Jakovičs, A., Baake, E. (2011). Statistical analysis of the influence of forces on particles in EM driven recirculated turbulent flows. *J. Phys.: Conference series*, 333, 1-14.

[4] Bhaga, D., Weber, M.E. (1981). Bubbles in viscous liquids: shapes, wakes and velocities. *J. Fluid. Mech.*, 105, 61-85.

[5] Kelley, E., Wu, M. (1997). Path instabilities of rising air bubbles in a Hele-Shaw cell. *Phys. Rev. Letters*, 79, 1265-1268.

[6] Roig, V., Roudet, M., Risso, F., Billet, A.-M. (2012). Dynamics of high-Reynolds-number bubble rising within a thin gap. *J. Fluid Mech.*, 707, 444-466.

[7] Zhang, C., Eckert, S., Gerbeth, G. (2005). Experimental study of single bubble motion in a liquid metal column exposed to a DC magnetic field. *Int. J. Multiphase Flow*, 31, 824-842.

[8] Lahjomri, J., Caperan, P., Alemany, A. (1993). The cylinder wake in a magnetic fild aligned with velocity. *J. Fluid. Mech.*, 253, 421-448.

[9] Shibasaki, Y., Ueno, K., Tagawa, T. (2010). Computation of a rising bubble in an enclosure filled with liquid metal under vertical magnetic fields. *ISIJ Int.*, 50, 363-370.

[10] Hua, J., Lou, J. (2007). Numerical simulation of bubble rising in viscous liquid. *J. Comput. Phys.*, 222, 769-795.